Ultrafast room-temperature crystallization of TiO2 nanotubes exploiting water-vapor treatment

SCIENTIFIC REPORTS

OPEN

SUBJECT AREAS:
NANOSCALE MATERIALS
SYNTHESIS AND PROCESSING

Received
2 October 2014

Accepted
9 December 2014

Published
15 January 2015

Correspondence and requests for materials should be addressed to A.L. (andrea.lamberti@polito.it)

Ultrafast Room-Temperature Crystallization of TiO_2 Nanotubes Exploiting Water-Vapor Treatment

Andrea Lamberti[1], Angelica Chiodoni[2], Nadia Shahzad[1], Stefano Bianco[2], Marzia Quaglio[2] & Candido F. Pirri[1,2]

[1]Department of Applied Science and Technology, Politecnico di Torino, C.so Duca degli Abruzzi 24, 10129 Turin, Italy, [2]Center for Space Human Robotics @Polito, Istituto Italiano di Tecnologia, Corso Trento, 21, 10129 Turin, Italy.

In this manuscript a near-room temperature crystallization process of anodic nanotubes from amorphous TiO_2 to anatase phase with a fast 30 minutes treatment is reported for the first time. This method involves the exposure of as-grown TiO_2 nanotubes to water vapor flow in ambient atmosphere. The water vapor-crystallized samples are deeply investigated in order to gain a whole understanding of their structural, physical and chemical properties. The photocatalytic activity of the converted material is tested by dye degradation experiment and the obtained performance confirms the highly promising properties of this low-temperature processed material.

Since the first report of Zwilling and coworkers[1], vertically aligned titanium dioxide (TiO_2) nanotube (NT) arrays by anodic oxidation have been largely investigated as active element for dye-sensitized solar cells[2–4], Li-ions batteries[5,6], water photoelectrolysis[7], artificial photosynthesis[8], biomedical devices[9,10], molecular sensors[11–13], gas sensors[14], and photocatalytic degradation of pollutants[15]. Thanks to their quasi one-dimensional arrangement, TiO_2 NTs are able to provide high surface area and superior electron transport properties resulting in a performance enhancement in the different fields of application. The electrochemical oxidation of Ti foil in a fluorine-based electrolyte (see Figure 1a) is a simple, cheap and green process, easy to be scaled up towards massive production and with a low energy payback time if used for energy harvesting applications. However, the as-grown NTs are fully amorphous, while crystalline TiO_2 is highly desired for most applications[16]. Thus, the nanotube synthesis is usually followed by a thermal annealing process (at around 450°C)[17] or by a hydrothermal treatment (at about 200°C)[18] to obtain a nanocrystalline material in the anatase phase. These additional treatments drastically affect the energetic balance of the overall process and dictate some constrains for the applicability of this material. In particular, the involved temperatures hinder the integration of ordered NT carpets on the most common polymeric substrates, which is a crucial step for the fabrication of flexible and lightweight devices.

For these reasons low-temperature water-assisted treatment to crystallize amorphous TiO_2 nanotubes have attracted enormous interest in the scientific community in the last years. All the proposed approaches are based on the interaction of the amorphous TiO_2 NT with water molecules and, depending on the interface that is formed, they can be divided in two main groups: solid-liquid and solid-gas interface reactions[19]. The former have been deeply investigated[18,20–23], revealing a crystallization rate and morphology modification which depend on the water temperature and incubation time. On the contrary, the latter approach is up to now less explored, even if the recent report of Liu and co-workers show that outstanding material properties can be obtained following this direction[19]. However, all the above mentioned methods required hydrothermal reaction conditions (high pressure and temperatures greater than 100°C)[18,20–22] or time-consuming incubation at room temperature (more than 72 hours in ambient atmosphere)[23] to obtain the desired anatase phase.

Herein we demonstrate for the first time to the best of our knowledge the near-room temperature (50°C) crystallization process of anodic NTs from amorphous TiO_2 to anatase phase after only 30 minutes of sample exposure to water vapor in ambient condition. The water vapor treated samples were deeply characterized in order to gain a whole understanding of their structural, physical and chemical properties, while their functional properties were evaluated in terms of their photocatalytic response during dye degradation experiments. The photocatalytic activity is a crucial characteristic, since it is the basis of a huge number of applications including for

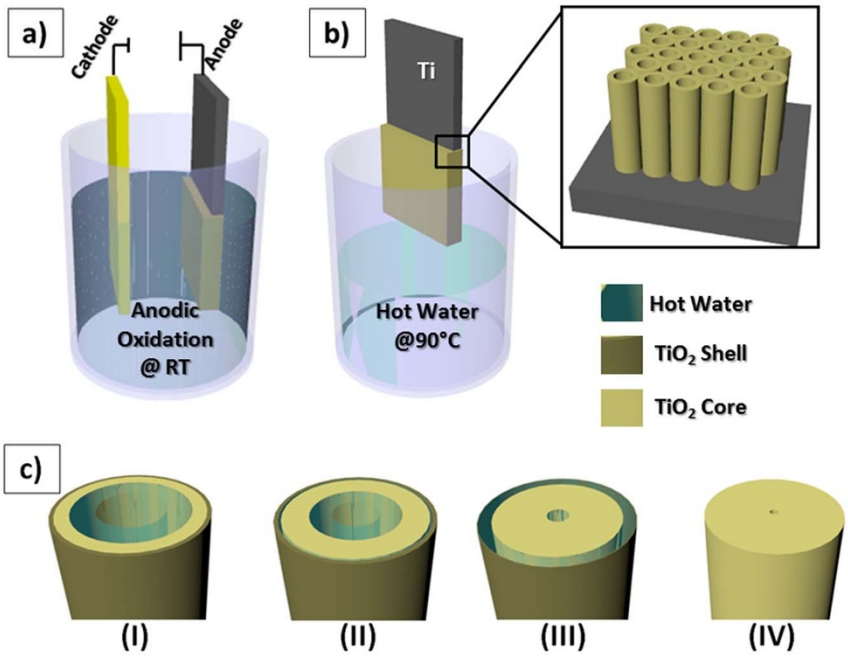

Figure 1 | Scheme of the experimental set-up used for the growth of the TiO_2 NTs (a) and for the water vapor crystallization (b); 3D representation of the crystallization/conversion process of TiO_2 from amorphous NTs to crystalline rod-like structures (c).

instance water splitting for the production of molecular hydrogen, photoreduction of CO_2, self-cleaning coatings, degradation or oxidization of organic contaminants, elimination of heavy metal ions, electrochromic devices, sensors, antibacterial surfaces and electrochemical solar cells. The obtained results confirm the effectiveness of the proposed ultrafast near-room temperature crystallization method.

Results and Discussion

The interaction of a solid surface exposed to water vapor is a highly complex interfacial system, since three phases (gas, liquid, and solid) and their interfaces (solid/liquid, liquid/gas and solid/gas) are involved. The low temperature crystallization approach proposed up to now can be described taking into account only the solid/liquid or solid/gas interfaces, and neglecting the presence of gas and liquid phases at the same time. Recently, Wang and coworkers showed that the conversion of amorphous nanotube array into polycrystalline TiO_2 is possible at room temperature exploiting spontaneous water-assisted reaction, based on sample incubation in DI-water for more than 72 hours[23]. This crystallization mechanism involves the dissolution and precipitation processes in which a spatial atomistic order is induced by water molecules. Nevertheless very long incubation time is required to obtain the full crystallization of the material. Other research groups investigated the effect of the hydrothermal treatment showing that faster conversion can be obtained increasing the reaction temperature under pressure[18,20–22]. On the contrary, our approach is based on the simple exposure in ambient atmosphere of as-grown amorphous TiO_2 NTs to the steam evolving by hot water (see Figure 1b). In general, the exposure of the metal oxide surface to water vapor leads to the formation of a thin water adlayer with a thickness on the order of nanometers that corresponds to the reversible adsorption and desorption of water from the surface. This aqueous film is the dynamic medium in which the crystallization process occurs.

It is necessary to specify that the as-grown TiO_2 NTs are composed by two layers (see Figure 1c step I): an outer part (shell) of pure and dense TiO_2 and an inner porous part (core) that contains incorporated electrolyte components[24]. In Figure 2 and Figure 3 we show the Field Emission Scanning Electron Microscopy (FESEM) and Transmission Electron Microscopy (TEM) images respectively, taken at different times of steam exposure. By increasing the exposure time, the NTs morphology evolves from an amorphous tubular shape up to a polycrystalline rod-like form. The possible conversion mechanism has been previously described by Wang et al.[23], but in our case it is accelerated by water vapor adsorption/condensation kinetics thanks to the formation of a solid/liquid/gas dynamic equilibrium. Two parallel events occur during the crystallization process. The first takes place at the inner tube walls, where the water vapor can condensate as hot water, acting as catalyzer in the crystallization process. Water molecules act as catalyzers favoring the rearrangement of TiO_6^{2-} octahedra in the amorphous TiO_2 nanotubes through hydration/dehydration reactions, as previously reported by Yu and coworkers[18]. The hot water cools down because of the lower temperature (equal to 50°C, accurately measured by Pt100 temperature detector) of the sample and it is substituted by new condensated molecules. The second process is the crystallization at the outer wall, where small crystals form at the NT surface at the very beginning.

In Figure 2, the image at 0 minutes shows the morphology of the as-grown NTs (corresponding to step I in Figure 1c). The amorphous nature of this material is demonstrated by the TEM characterization, image at 0 minutes in Figure 3. After 5 minutes of exposure, some crystallites appear at the outer surface of the tubes that increase after 10 minutes, when the formation of crystals in the inner shell of the tube becomes also evident.

After 20 minutes, the formation of a core-shell structure is the ultimate step (step II in Figure 1c) before the dissolution of the shell by the thickness reduction of the pristine amorphous wall in favor of the consolidation of the inner rod-like structure. This consolidation process is well visible starting from 30 minutes of exposure time, where the conversion process into the porous rod-like structure is almost completed, even if a residual thin wall remains (step III in Figure 1c). This residual wall decreases in thickness as the exposure time increases, until its complete dissolution (step IV in Figure 1c). The grain size, evaluated from FESEM characterization, seems to be unvaried starting from the sample exposed for 30 minutes, up to the one exposed for 4 hours. A more precise estimation of the grain size is given by the High Resolution TEM (HRTEM) image reported in

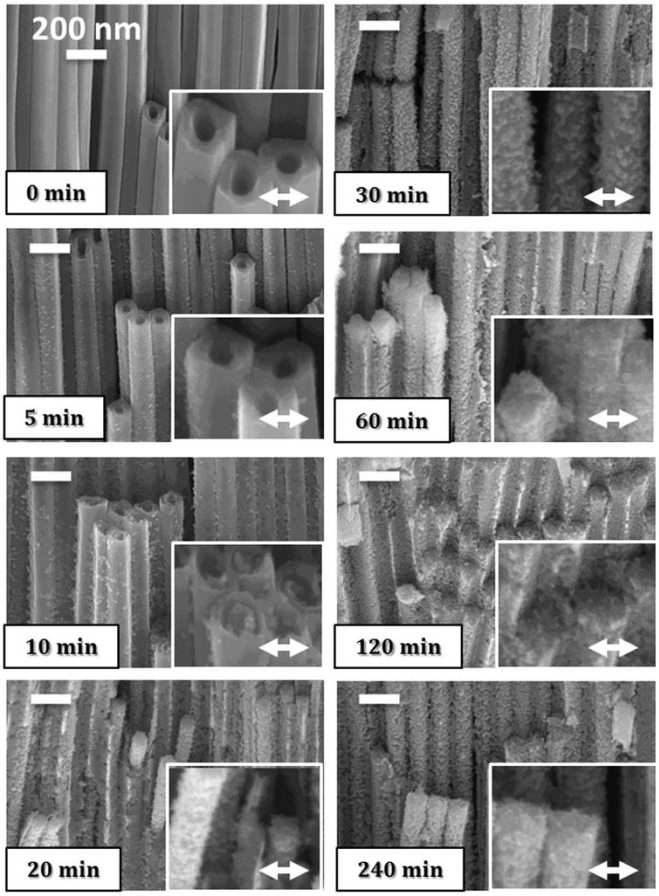

Figure 2 | FESEM images showing the evolution in the morphology of TiO_2 NT array as a function of the water vapor exposure time from 0 up to 240 minutes (the insets show higher magnifications in order to better appreciate the conversion from nanotubes to nanorods, the scale arrows are equal to 100 nm).

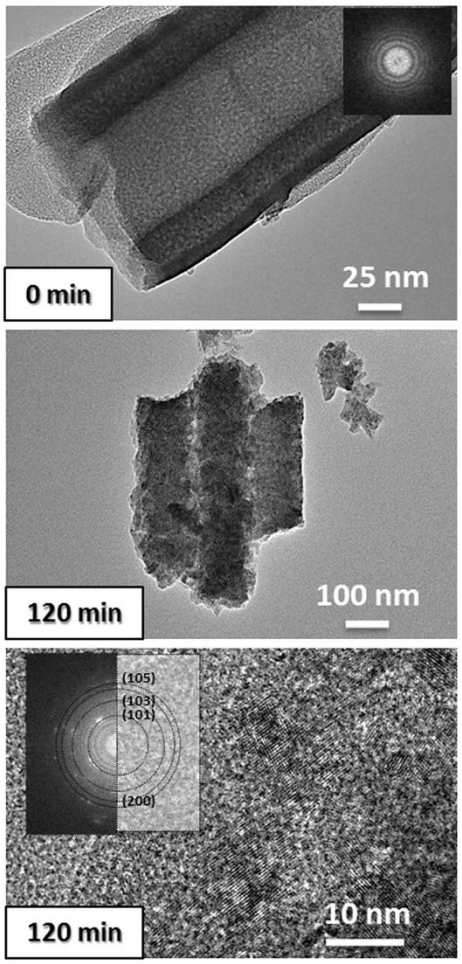

Figure 3 | Bright Field TEM and HRTEM characterization of the pristine TiO_2 nanotubes (0 min) and after 120 minutes of exposure time. The insets show the Fast Fourier Transform patterns.

Figure 3, and it is in the range of 5–10 nm. The Fast Fourier Transform (FFT) in the inset of the same image demonstrates the polycrystalline-randomly oriented nature of the anatase rod-like structure obtained after 2 hours of exposure time, in agreement with the X-Ray Diffraction (XRD) results reported below and in the Supporting Information (Figure S3).

The porous nature of the converted TiO_2 is also confirmed by BET (Brunauer–Emmett–Teller) measurements. In fact the calculated specific area, evaluated by nitrogen sorption isotherm, increases with the water vapor treatment according to the FESEM observation. The amorphous nanotube array exhibits about 38 m^2/g surface area, while after 2 hours of steam exposure its value is increased up to 106 m^2/g, with a reduction of the pore size from about 12 nm down to about 4 nm (see Figure S4).

Crystallographic data confirm that just after anodization the TiO_2 nanotubes are amorphous, but a rapid structural evolution emerges during the solid/liquid/vapor interaction. As evidenced in the XRD spectra reported in Figure 4a, the crystallization of the material in the anatase form starts rapidly, and after a 10 min treatment the main diffraction peak at 25.3 deg (2 theta), related to the (101) crystal face, begins to be visible. For longer vapor exposure, an ultrafast crystallization kinetic is evidenced, and the crystallization process saturates after 30 min of treatment. This aspect is well evidenced by the evolution of the average crystallite size, estimated through the Scherrer formula, as a function of the vapor exposure time, reported in Figure 4b. The average crystallite dimension is approximately equal to 7 nm after 30 min treatment and does not evolve significantly for longer water vapor exposure, in line with the HRTEM analysis.

It is important to underline that no intentional heating was provided to the substrates but, due to the interaction with the water vapor, a slight increase of the temperature of the substrate was evidenced, reaching the maximum value of 50°C. In order to exclude this mild heating of the substrate as potential responsible of the fast crystallization process, other as-grown TiO_2 NT sample were prepared on purpose and incubated into hot water at 50°C for different times up to 4 hours (see Supporting Information). Neither the FESEM characterization (Figure S1) nor the XRD analysis (Figure S2) evidenced any morphological or crystallographic evolution during this treatment. These results are in line with the observation reported by Krengvirat and co-workers that demonstrated a minimum temperature of crystallization equal to 70°C with 3 hours of treatment[22]. Our empirical evidence supports the hypothesis that the rapid formation of anatase phase can be only due to the interaction of water vapor molecules with the amorphous TiO_2 nanotube walls. Unlike what happens in the liquid water, the molecules in the gas are not in strong interaction with each other. This allows greater freedom to the water molecules to fill better and faster a nanoporous structure as the TiO_2 NTs. Consequently they can increase the adsorption rate onto the amorphous titania surface, dramatically increasing the rate of crystallization.

Contact angle (CA) measurements were performed to study the evolution of TiO_2 nanotubes wettability depending on the water vapor exposure time (see Figure 4c). The mean value of the water

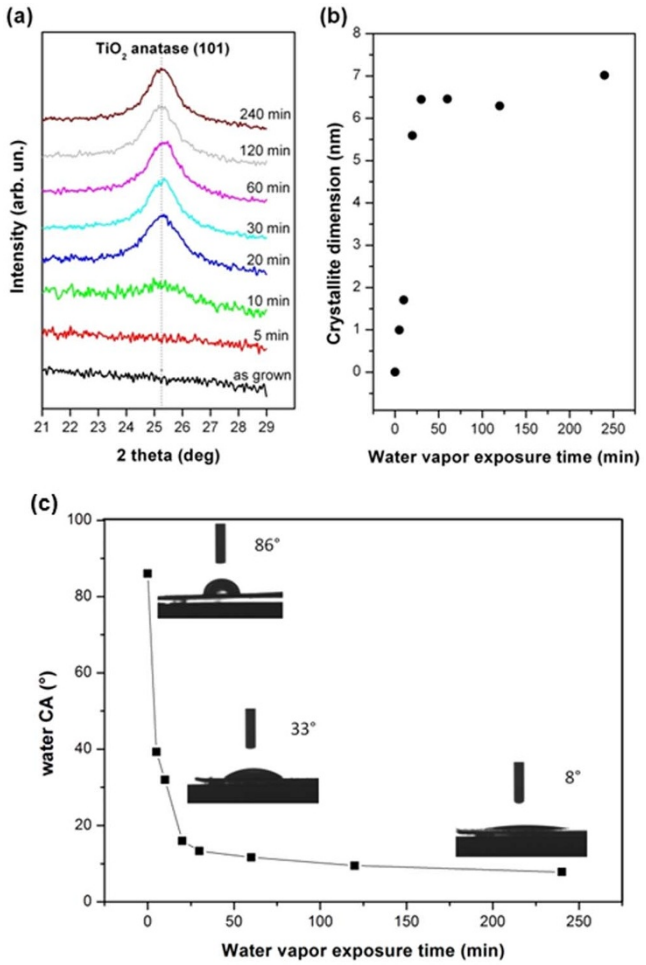

Figure 4 | Evolution of the main anatase X-ray diffraction peak ((101) crystal face) during the water vapor exposure (a). Average crystallite size, estimated through the Scherrer equation, for different water vapor exposure times (b). Water contact angle values recorded at incremental water-vapor exposure time (c).

CA exponentially decreases from slightly hydrophobic for the amorphous nanotubes to super hydrophilic in the water-crystallized material. This trend follows and confirms the increase of the surface roughness revealed by FESEM and BET investigations. The enhanced wettability can be ascribed to the water vapor interaction, which is responsible for the introduction of a high number of surface defects, acting as adsorption sites for –OH groups. Furthermore, this increased wetting behaviour can be considered as a co-responsible for the rapid crystallization of the material during the interaction with the water vapor. In fact, the steam exposure significantly increases the wettability and consequently the interaction between water (catalyzing agent of crystallization) and the surface of TiO_2 (gradually more and more crystalline) gets stronger. As counterproof also the contact angle of the nanotube sample incubated in water at 50°C was measured and the results show that no considerable variations of wettability can be observed.

The influence of vapor treatment on the chemical structure of TiO_2 NT arrays was investigated by Fourier Transform-InfraRed (FT-IR) analysis, and the related spectra are shown in Figure 5a. The main results are well in line with those shown by Krengvirat and coworkers[22]. A broad band at about 3400 cm^{-1} and a weak band at 1626 cm^{-1} are present at different extent in all the samples, and they can be ascribed to chemisorbed H_2O. In the as-grown material several peaks are present, that can be related to the chemicals used during the anodization step. A weak band associated to –OH groups is visible at 1433 cm^{-1}. Stretching vibrations consistent with amino-acids ($-NH_3^+$) were detected at 1072 cm^{-1}, and N–H deformation vibration is well visible at 1558 cm^{-1}. The weak bands at 854 and 610 cm^{-1} are attributed to the stretching vibration of Ti–O in the TiO_6 octahedron. After water vapor treatment, a broad band appears in all the samples at about 2900 cm^{-1}, and it is consistent with the degradation of organic compounds associated to the dissolution of residual ethylene glycol. The disappearance of the bands located at 1558 and 1072 cm^{-1} confirmed the removal of adsorbed ammonium. In the treated samples the water and –OH related bands, at 1626 cm^{-1} and 1433 cm^{-1} respectively, become stronger with increasing treatment time, which is in line with the progressively increased wettability of the material.

Moreover, to further analyze the crystallization process, Raman spectroscopy was employed. Figure 5b displays Raman spectra of the TiO_2 nanotubes in the as-grown condition and after the water vapor treatment for different exposure times. The as-grown sample exhibits three very broad bands confirming the presence of amorphous structure of TiO_2. Such broad features are assigned to the Ti–O bending (190 cm^{-1}, 450 cm^{-1}) and Ti–O stretching (610 cm^{-1}) vibrations. An additional broad shoulder appears at 890 cm^{-1}, followed by a series of vibrational bands of variable intensity at 1075, 1136, 1205, 1283, 1370, 1456 and 1595 cm^{-1}. These bands existing in the range 1000–1700 cm^{-1} as well as the broad shoulder at 895 cm^{-1} are closely related to the Raman modes of ethylene glycol molecules as observed by Likodimos et al.[25] and after 30 minutes of water vapor exposure are found disappeared. The obtained Raman active modes at ~150 cm^{-1}, 200 cm^{-1}, 399 cm^{-1}, 513 cm^{-1} and 633 cm^{-1} are related to the tetragonal structure of anatase TiO_2 with D4h space group[26].

The influence of water vapor treatment on the optical properties of TiO_2 NTs was investigated and the results are reported in Figure 5c. Absorbance of as-grown nanotubes increases in visible region from higher wavelengths to lower ones and the absorption edge is not well-defined and less sharp, a characteristic behavior of amorphous oxides[27]. Nevertheless after 30 minutes of water vapor treatment, nanotube arrays showed comparatively flat curve in visible region and a sharp absorption edge indicating the improved crystallinity of the material.

The indirect energy band gap (E_g) for the water-vapor crystallized TiO_2 nanotubes, has been determined by extrapolation of the plot of $(F(R)*h\upsilon)^{1/2}$ against the photon energy, $h\upsilon$, according to the following equation: $F(R)*h\upsilon = const\ (h\upsilon - E_g)^2$. The obtained value of the semiconductor band gap, i.e. 3.27 ± 0.01 eV, is very close to the values (3.26–3.30 eV) reported by other researchers for anatase phase[28–30], which is considered the best phase of titania for photocatalytic applications[31]. This result shows that the optical properties analyzed by UV-Vis spectroscopy are clearly related to the crystalline phase obtained from Raman and XRD measurements.

Finally we evaluated the decomposition of methylene blue (MB) dye under UV light as test to assess the photocatalytic activity of the prepared samples. The photocatalytic degradation and mineralization of the dye in aqueous solution is a well-known process[32–34], thus it could be considered a valuable protocol to test the properties of the synthesized material.

In Figure 6a the trend of the ratio C/C_0 versus time is reported, where C_0 is the concentration of starting MB solution in water and C is the one after the illumination. In general, the degradation of dyes depend on several parameters such as solution pH, catalyst concentration, substrate morphology, etc. In our case, we compared the decomposition kinetics under the same experimental conditions, revealing a first-order Langmuir–Hinshelwood process, as witnessed by the linear plot reported in the Supporting material (Fig. S5). Since the decomposition rate is proportional to the surface coverage, we argued that the improved photocatalytic properties of the water

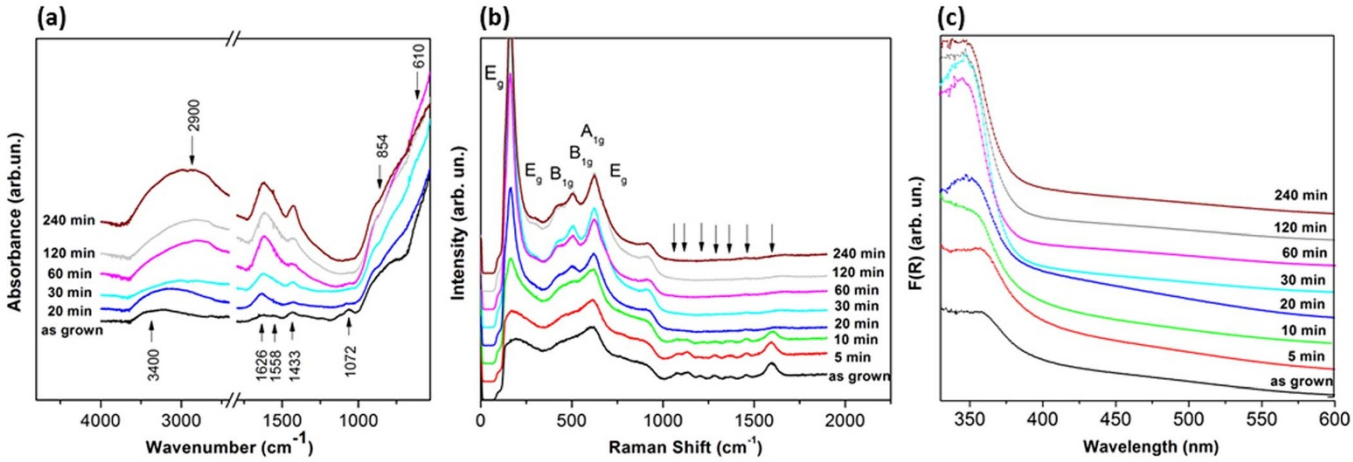

Figure 5 | ATR FT-IR (a), Raman (b) and UV-Vis (c) spectra of TiO_2 NTs acquired at different time of exposure to water vapor.

vapor- treated TiO_2 with respect to the other nanocrystalline titania-based materials are related with the higher exposed surface area (as measured by BET). Given that for an effective applicability a photocatalyst should be stable under repeated uses, the photocatalytic stability of water vapor crystallized TiO_2 NTs was verified testing the samples repeatedly five times. As shown in Figure 6b, after being cleaned, dried, and then recycled, the photocatalysts exhibit almost the same degradation of MB dye under the selected reaction conditions, with only a 5% reduction after 5 consecutive cycles.

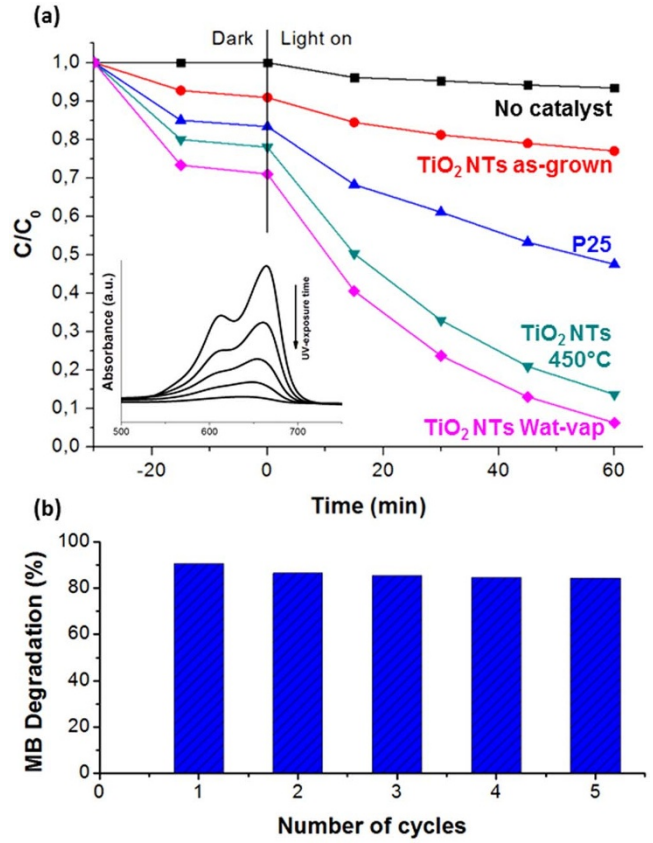

Figure 6 | The photocatalytic decomposition of methylene blue aqueous solution under UV light obtained comparing as-grown, heat treated (450°C) and water vapor NTs is shown (a). MB degradation without catalyst presence and with P25 powder are reported as comparison. The inset shows the UV-Vis absorbance spectrum of MB solution at different recorded times of illumination using the water vapor treated NTs. Cycling runs for MB degradation after 60 minutes of UV illumination (b).

Conclusions

In summary, we demonstrated for the first time that amorphous TiO_2 NTs can be crystallized into anatase phase after exposure to water vapor in ambient condition. This facile approach provides a cost effective strategy to allow the integration of ordered NT carpets on temperature-sensitive substrates, as crucial step for the fabrication of flexible and lightweight devices. We found that the crystallographic conversion is complete after only 30 minutes, with physical and chemical properties of the NTs that remains unvaried for prolonged treatment. Finally the photocatalytic activity of the converted material was tested by dye degradation experiments, revealing an improvement with respect to thermally treated samples, and demonstrating the effectiveness of the here proposed crystallization method.

Experimental

Materials and methods. TiO_2 nanotube arrays were grown by anodic oxidation of Ti foil (250 μm thick, 99.6% purity, Goodfellow) in an electrolytic solution consisting of 0.5 wt% NH_4F (98%, Sigma Aldrich) and 2.5 vol% deionized water in ethylene glycol (98%, Sigma Aldrich). Samples were cleaned by ultrasonication in acetone, rinsed in ethanol and pretreated into a 1wt% HF aqueous solution to remove the native oxide layer obtaining a fresh metal surface for the NTs growth. A Pt sheet (250 μm thick, 99.99% purity, Goodfellow) was employed as a cathode in a two-electrode configuration Teflon cell. The electrochemical process was conducted under continuous stirring at ambient temperature applying an anodization potential of 60 V using a DC power supply (GW Instek SPD-3606). After the anodization, the oxidized Ti foils were abundantly rinsed in DI-water to remove the impurities eventually adsorbed from the electrolytic solution during the growth.

The NT arrays were subsequently fixed into a clamping system and exposed to the water vapor evolving by DI-water (18.2 $M\Omega \cdot cm^{-1}$ @ 25°C) previously heated at 90°C by an hot plate for different times (0–240 min). The temperature of the substrate was measured by a Pt100 temperature detector connected to a dedicated controller.

Characterization. The evolution of the morphology on the different samples was characterized by a ZEISS Auriga FESEM. The TEM was performed with a FEI Tecnai F20ST operating at 200 kV, to evaluate the quality of the crystalline TiO_2 in Bright Field and High Resolution modes. For the TEM characterization, the sample was scratched from the substrate and dispersed in HPLC ultrapure ethanol for 2 minutes by sonication. Then, a drop of dispersion was put on a lacey carbon copper grid and let dry in ambient atmosphere.

X-ray diffraction patterns were acquired with a PANalytical X'Pert Pro equipment in Bragg-Brentano configuration (Cu Kα X-ray source). The average anatase crystallite size was estimated through the Scherrer equation using the main anatase peak, related with the (101) crystal planes. Its full width at half maximum was estimated with a pseudo-Voigt fitting and corrected taking into account the instrumental broadening.

Fourier transformed infrared spectra were recorded using a Nicolet 5700 FTIR Spectrometer in attenuated total reflectance (ATR) mode with 4 cm^{-1} resolution and an average of 64 scans.

The room temperature Raman spectra of NT arrays were collected using Renishaw Invia spectrometer with the 514 nm Ar-Kr excitation laser beam. Optical absorbance of the water vapor treated TiO_2 NT arrays was measured by a Varian Cary 5000 spectrophotometer employing integrating sphere.

Brunauer–Emmett–Teller specific surface area was measured from N_2 sorption isotherms (Quantachrome Autosorb1) by multipoint method within the relative pressure range of 0.1–0.3 P/P_0.

Contact angle measurements were performed using a OCA H200 Dataphysics equipment in ambient conditions. The sessile drop method was implemented employing DI-water droplets with 1.5 μl volume.

The photocatalytic activity of converted TiO_2 NT array was investigated by the incubation of a sample (with 1 cm^2 active area and thickness equal to 6 μm) into 20 mL methylene blue water solution (2×10^{-5} M) under UV illumination (30 mW/cm^2, LC8 Lightningcure, Hamamatsu) and measuring the absorbance spectra each 15 min up to 1 hour. Heat treated (450°C for 1 hour) TiO_2 NT arrays with the same area and thickness were used as comparison. The residual concentration of MB was evaluated by its optical absorbance peak intensity at 663 nm with a Varian Cary 5000 spectrophotometer.

1. Zwilling, V., Aucouturier, M. & Darque-Ceretti, E. Anodic oxidation of titanium and TA6V alloy in chromic media. An electrochemical approach. *Electrochim. Acta* **45**, 921–929 (1999).
2. Zhu, K., Neale, N. R., Miedaner, A. & Frank, A. J. Enhanced charge-collection efficiencies and light scattering in dye-sensitized solar cells using oriented TiO_2 nanotubes arrays. *Nano Lett.* **7**, 69–74 (2007).
3. Mor, G. K., Shankar, K., Paulose, M., Varghese, O. K. & Grimes, C. A. Use of highly-ordered TiO_2 nanotube arrays in dye-sensitized solar cells. *Nano Lett.* **6**, 215–218 (2006).
4. Lamberti, A. *et al*. Charge transport improvement employing TiO_2 nanotube arrays as front-side illuminated dye-sensitized solar cell photoanodes. *Phys. Chem. Chem. Phys.* **15**, 2596–2602 (2013).
5. Meekins, B. H. & Kamat, P. V. Got TiO_2 nanotubes? Lithium ion intercalation can boost their photoelectrochemical performance. *ACS Nano* **3**, 3437–3446 (2009).
6. Lamberti, A. *et al*. Vertically aligned TiO_2 nanotube array for high rate Li-based micro-battery anodes with improved durability. *Electrochim. Acta* **102**, 233–239 (2013).
7. Lee, K., Hahn, R., Altomare, M., Selli, E. & Schmuki, P. Intrinsic Au Decoration of Growing TiO_2 Nanotubes and Formation of a High-Efficiency Photocatalyst for H2 Production. *Adv. Mater.* **25**, 6133–6137 (2013).
8. Ryu, J., Lee, S. H., Nam, D. H. & Park, C. B. Rational Design and Engineering of Quantum-Dot-Sensitized TiO_2 Nanotube Arrays for Artificial Photosynthesis. *Adv. Mater.* **23**, 1883–1888 (2011).
9. von Wilmowsky, C. *et al*. In vivo evaluation of anodic TiO_2 nanotubes: an experimental study in the pig. *J. Biomed. Mater. Res. B* **89**, 165–171 (2009).
10. Popat, K. C., Eltgroth, M., LaTempa, T. J., Grimes, C. A. & Desai, T. A. Titania Nanotubes: A Novel Platform for Drug-Eluting Coatings for Medical Implants?. *Small* **3**, 1878–1881 (2007).
11. Roguska, A. *et al*. Raman investigations of TiO_2 nanotube substrates covered with thin Ag or Cu deposits. *Journal Raman Spectrosc.* **40**, 1652–1656 (2009).
12. Li, X., Chen, G., Yang, L., Jin, Z. & Liu, J. Multifunctional Au-Coated TiO_2 Nanotube Arrays as Recyclable SERS Substrates for Multifold Organic Pollutants Detection. *Adv. Funct. Mater.* **20**, 2815–2824 (2010).
13. Zheng, Q. *et al*. Self-Organized TiO_2 Nanotube Array Sensor for the Determination of Chemical Oxygen Demand. *Adv. Mater.* **20**, 1044–1049 (2008).
14. Şennik, E., Çolak, Z., Kılınç, N. & Öztürk, Z. Z. Synthesis of highly-ordered TiO_2 nanotubes for a hydrogen sensor. *Int. J. Hydrogen Ener.* **35**, 4420–4427 (2010).
15. Macak, J. M., Zlamal, M., Krysa, J. & Schmuki, P. Self-Organized TiO_2 Nanotube Layers as Highly Efficient Photocatalysts. *Small* **3**, 300–304 (2007).
16. Roy, P., Berger, S. & Schmuki, P. TiO_2 nanotubes: synthesis and applications. *Angew. Chem. Int. Edit.* **50**, 2904–2939 (2011).
17. Yu, J. & Wang, B. Effect of calcination temperature on morphology and photoelectrochemical properties of anodized titanium dioxide nanotube arrays. *Appl. Catal. B-Environ.* **94**, 295–302 (2010).
18. Yu, J., Dai, G. & Cheng, B. Effect of crystallization methods on morphology and photocatalytic activity of anodized TiO_2 nanotube array films. *J. Phys. Chem. C* **114**, 19378–19385 (2010).
19. Liu, J., Liu, Z., Zhang, T., Zhai, J. & Jiang, L. Low-temperature crystallization of anodized TiO_2 nanotubes at the solid–gas interface and their photoelectrochemical properties. *Nanoscale* **5**, 6139–6144 (2013).
20. Liao, Y., Que, W., Zhong, P., Zhang, J. & He, Y. A facile method to crystallize amorphous anodized TiO_2 nanotubes at low temperature. *ACS Appl. Mater. Interfaces* **3**, 2800–2804 (2011).
21. Liu, N., Albu, S. P., Lee, K., So, S. & Schmuki, P. Water annealing and other low temperature treatments of anodic TiO_2 nanotubes: A comparison of properties and efficiencies in dye sensitized solar cells and for water splitting. *Electrochim. Acta* **82**, 98–102 (2012).
22. Krengvirat, W. *et al*. Low-temperature crystallization of TiO_2 nanotube arrays via hot water treatment and their photocatalytic properties under visible-light irradiation. *Mater. Chem. Phys.* **137**, 991–998 (2013).
23. Wang, D. *et al*. Spontaneous phase and morphology transformations of anodized titania nanotubes induced by water at room temperature. *Nano Lett.* **11**, 3649–3655 (2011).
24. Albu, S. P. *et al*. Formation of Double-Walled TiO_2 Nanotubes and Robust Anatase Membranes. *Adv. Mater.* **20**, 4135–4139 (2008).
25. Likodimos, V., Stergiopoulos, T., Falaras, P., Kunze, J. & Schmuki, P. Phase composition, size, orientation, and antenna effects of self-assembled anodized titania nanotube arrays: A polarized micro-Raman investigation. *J. Phys. Chem. C* **112**, 12687–12696 (2008).
26. Arsov, L. D., Kormann, C. & Plieth, W. In situ Raman spectra of anodically formed titanium dioxide layers in solutions of H 2 SO 4, KOH, and HNO 3. *J. Electrochem. Soc.* **138**, 2964–2970 (1991).
27. Hogarth, C. A. & Nadeem, M. Y. The optical absorption edge in amorphous thin films of germania and of germania with barium oxide. *Phys. Status Solidi A* **68**, K181–K184 (1981).
28. Aarik, J., Aidla, A., Kiisler, A.-A., Uustare, T. & Sammelselg, V. Effect of crystal structure on optical properties of TiO_2 films grown by atomic layer deposition. *Thin Solid Films* **305**, 270–273 (1997).
29. Zhang, X. *et al*. Construction of Self-Supported Three– Dimensional TiO_2 Sheeted Networks with Enhanced Photocatalytic Activity. *Sci. Rep.* **3**, 1–6 (2013).
30. Grimes, C. A. & Mor, G. K. Material Properties of TiO_2 Nanotube Arrays: Structural, Elemental, Mechanical, Optical and Electrical. In *TiO_2 Nanotube Arrays*. Springer US. 67–113 (2009).
31. Luttrell, T. *et al*. Why is anatase a better photocatalyst than rutile? - Model studies on epitaxial TiO_2 films. *Sci. Rep.* **4**, 1–8 (2014).
32. Houas, A. *et al*. Photocatalytic degradation pathway of methylene blue in water. *Appl. Catal. B: Environ.* **31**, 145–157 (2001).
33. Yang, Y., Zhang, G. & Xu, W. Facile synthesis and photocatalytic properties of Ag-AgCl-TiO_2/rectorite composite. *J. Colloids Interface Sci.* **376**, 217–223 (2012).
34. Fujishima, A., Zhang, X. & Tryk, D. A. TiO_2 photocatalysis and related surface phenomena. *Surf. Sci. Rep.* **63**, 515–582 (2008).

Acknowledgments

Authors would like to thank Miss C. Ottone for the aid in BET measurements and Dr. A. Sacco and Dr. G. Cicero for the fruitful discussions.

Author contributions

A.L. conceived the idea, performed the growth and the crystallization of NT arrays, performed the contact angle characterizations and the photochatalitic degradation experiments, and wrote the paper. A.C. performed FESEM and TEM characterization. N.S. performed Raman and Optical measurements. S.B. performed XRD measurements and the Sherrer analysis. M.Q. performed FTIR measurements. C.F.P. supervised the activity. All authors contributed to the scientific discussion and revision of the article, giving approval to the final version of the manuscript.

Additional information

Supplementary information accompanies this paper at http://www.nature.com/scientificreports

Competing financial interests: The authors declare no competing financial interests.

How to cite this article: Lamberti, A. *et al*. Ultrafast Room-Temperature Crystallization of TiO_2 Nanotubes Exploiting Water-Vapor Treatment. *Sci. Rep.* **5**, 7808; DOI:10.1038/srep07808 (2015).